Oaxaca Coast

Part 2
COASTAL SEDIMENT PROBLEMS

Michoacan Coast

CHAPTER 11

FLUME EXPERIMENTS ON SAND TRANSPORT BY WAVES AND CURRENTS

Douglas L. Inman
Scripps Institution of Oceanography,
University of California, La Jolla, California

and

Anthony J. Bowen
Hydraulics Research Station, Wallingford, England

ABSTRACT

Measurements were made of the sand transport (solid discharge) caused by waves and currents traveling over a horizontal sand bed in water 50 cm deep. The waves had heights of 15 cm, and periods of 1.4 and 2.0 sec. The sand transport was measured first in the presence of waves only, then in the presence of waves superimposed on currents. The currents flowed in the direction of wave travel, with steady uniform velocities of 2, 4, and 6 cm/sec.

Since sand moves to and fro under the influence of waves, sand traps were placed flush with the surface at either end of the bed. The net sand transport was determined by subtracting the amount of sand trapped at the upwave end of the bed, from that trapped at the downwave end.

The total amount of sand caught in both traps was greatest with waves of 2.0 sec period, while the net sand transport was greatest with waves of 1.4 sec period. Super position of waves on currents of 2 cm/sec produced a two-fold increase in the sand transport for both wave types. Surprisingly, faster currents of 4 and 6 cm/sec caused the discharge to decrease somewhat.

Estimates of the power expended by waves was obtained from the decrement in wave height as the wave traveled over the sand bed. The decrement in wave height was found to be about 10^{-3} per unit of distance traveled. Certain calculations show that about one tenth of the total power expended by the waves was used in transporting sediment.

INTRODUCTION

Surface waves traveling in shallow water over a horizontal bed of sand usually produce a net transport of sand in the direction of wave travel. As a working hypothesis it was assumed that the wave motion made the sand available for transport, so that any current near the bed would produce a net transport of sand. The purpose of this experiment was to test the hypothesis by measuring the transport rates of sand under

Contribution from the Scripps Institution of Oceanography, University of California, San Diego.

several types of waves and for a variety of superimposed currents.

The purpose of the superimposed current was to simulate conditions prevailing along natural beaches. Longuet-Higgins (1953) and Russell and Osorio (1958) have shown theoretically and practically that, in a flume, the wave-induced drift velocity is downwave near the surface and bed but upwave in the center. However experiments on real beaches, Shepard and Inman (1950), have shown that the drift velocity is onshore at all depths; the system being kept in equilibrium by the rip currents spaced along the beach. To obtain a model of the conditions which prevail between the rip currents it was considered necessary to superimpose a current upon the wave system in the flume. The current velocities superimposed were of the same order of magnitude as the wave-induced drift velocities, i.e., several cm/sec.

It is assumed that a portion of the wave power is expended on the granular bed by the to and fro motion of the water over the bed, and that this power places the sand grains in motion and supports their weight above the bed. If the back and forth motions are equal, then there should be no net transport of grains and the wave power is simply expended in to and fro motion of the sand. Since the grains are supported above the bed by the wave stresses, the presence of a current should produce a transport in the direction of the current. A relation of this sort for wave induced transport was formulated by Bagnold (in press, eq. 10).

$$i_\theta = K\omega \frac{u_\theta}{u_m} \quad \ldots\ldots\ldots\ldots\ldots (1)$$

where i_θ is the dynamic transport rate of sand (i.e., immersed weight per unit time and per unit width of bed) which results when wave stress (ω/u_m) places sand available for transport in the presence of a current u_θ, and K is a dimensionless coefficient of proportionality. In a sense K is a measure of efficiency, which conceivably could have values exceeding unity. In this relation, ω is the decrement in transmitted power of the waves attributable to bed drag, and u_m is the maximum horizontal component of the orbital velocity near the bed.

The dynamic transport rate i_θ is equal to g'mU where $g' = \frac{\rho_s - \rho}{\rho_s} g$ is a factor converting the dry mass transport rate per unit width mU into immersed weight transport, g is the acceleration of gravity, m is the mass of sediment load over unit area of bed which is transported at velocity U and ρ and ρ_s are the density of the liquid and solid grains respectively. Thus the dry mass transport rate of sand in grams per cm width of wave crest per second becomes

$$j = mU = K\omega \frac{u_\theta}{u_m} \frac{1}{g'} \quad \ldots\ldots\ldots (2)$$

where u_θ is a steady current flowing near the bed in the direction of wave travel.

Longuet-Higgins and Stewart (1960) show that when a train of gravity waves of height H, ride upon a steady current $\bar{u}$, the whole power transmitted forward across any vertical plane normal to the motion is given by

$$P = ECn + E\bar{u} + \tfrac{1}{2}\rho h\, \bar{u}^3 + S_x\bar{u} \quad \ldots . (3)$$

where $E = \frac{1}{8}\rho g H^2$ is the mean energy density of the waves per unit surface area, Cn is the group velocity of waves in still water of depth h, and S_x is the radiation stress defined below. The first two terms represent the bodily transport of wave energy by the group velocity and the stream velocity, while the third term represents the transport by the stream of its own kinetic energy. The last term represents the work done due to the interaction of waves and currents and is equal to

$$S_x = E\left[2n - \tfrac{1}{2}\right] \ldots\ldots\ldots\ldots (4)$$

where n is the ratio of the wave group velocity Cn to the wave phase velocity C.

The decrement in wave power per unit of bed area, ω, is equal to dP/dx, which for waves propagating in water of constant depth and hence at constant velocity, becomes

$$\omega = \frac{dP}{dx} = \tfrac{1}{4}\rho g H \frac{dH}{dx}\left[Cn + U\,(2n + \tfrac{1}{2})\right] . \quad (5)$$

where the third term in equation (3) is assumed to be negligible. If there is no current, then the relation becomes $\omega = \frac{1}{4}\rho g H \frac{dH}{dx} Cn$.

An estimate of the decrement in transmitted power ω can be obtained from relation (5) if the decrement in wave height per unit of distance traveled, dH/dx, is known. A primary objective of these experiments was to obtain experimental values of dH/dx over rippled and smooth bed.

It was observed that the distribution in wave height was approximately exponential in form and could be represented by

$$H = H_1 e^{-ax} \ldots\ldots\ldots\ldots\ldots (6)$$

where H is the wave height at some distance x downwave from an incident wave of height H_1, and "a" is a wave attenuation coefficient with units of x^{-1}. Differentiation of this relation gives the decrement in wave height as dH/dx = -aH. In the analysis of the experimental data in a smooth channel it was assumed that the total attenuation coefficient, a, was the sum of the attenuations due to viscous effects on the smooth wall (a_1) and smooth bottom (a_2). In the presence of a sand bed it was assumed that the total attenuation coefficient was the sum of a_1 and the attenuation due to the rippled sand bottom a_3, i.e., in the absence of a smooth bed $a = a_1 + a_2$ and in the presence of a rippled bed $a = a_1 + a_3$.

In the case of waves traveling in a channel bounded by a smooth bed and side walls, the motion in the boundary layers should be laminar. It would be expected that viscous stresses in the thin laminar layer near the solid boundary would account for most of the energy dissipation. A calculation by Hunt (1952) making plausible assumptions, gives the relation for the theoretical wave attenuation coefficient as

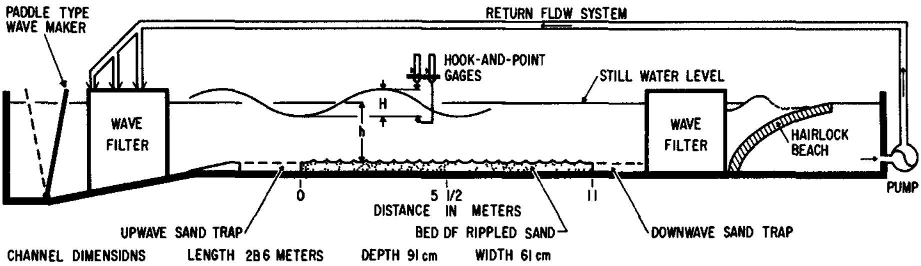

Fig. I. Schematic diagram of the wave channel.

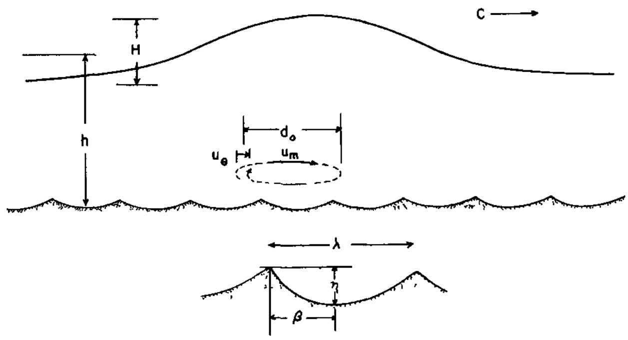

Fig. 2. Schematic diagram of wave and bed features.

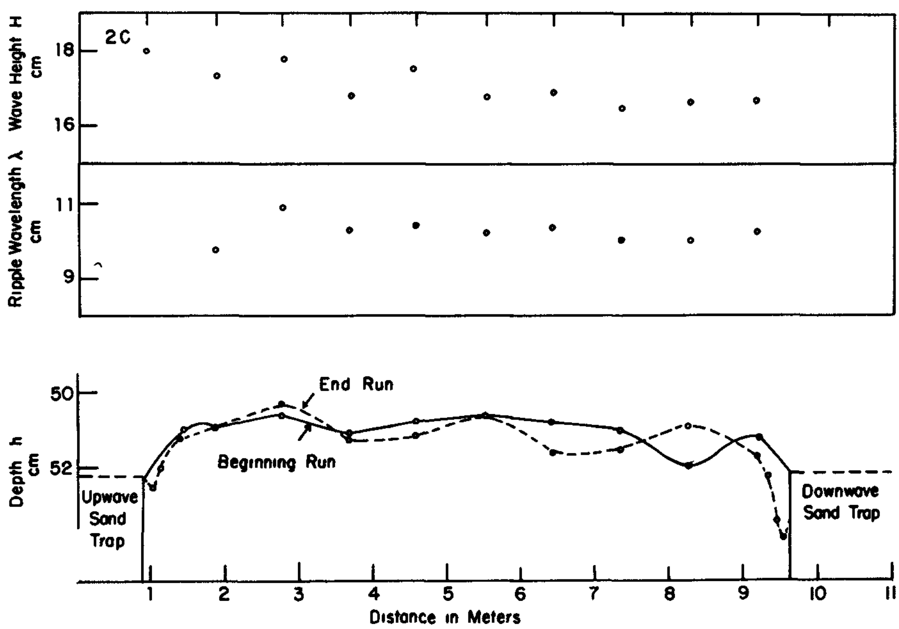

Fig. 3. Comparison of bed profiles, Run 2C.

$$a_o = \frac{k}{b}\left[\frac{\nu T}{\pi}\right]^{\frac{1}{2}}\left[\frac{kb + \sinh 2kh}{2kh + \sinh 2kh}\right] \quad \ldots\ldots (7)$$

where $k = 2\pi/L$ is the wave number, b is the width of the channel, ν is the kinetic viscosity, and h is the still water depth.

EQUIPMENT

The experiments were performed in the "94-foot wave channel" at the Hydraulic Research Station of the Department of Scientific and Industrial Research, Wallingford, England. Waves are generated in the deep end of the concrete channel by a paddle-type wave maker, and propagate into a uniform section of channel, 21 meters long by 91 cm deep and 61 cm wide (Figure 1). An inclined beach, consisting of a three inch thick porous "hair-lock" mat, was placed at the downwave end of the channel to absorb the energy of the waves and minimize their reflection. To decrease wave harmonics, filters consisting of eight vertical, slightly wavy sections of perforated metal were situated near the wave maker and the hair-lock beach. When desired, a steady current of 2 to 6 cm/sec was generated by pumping water from behind the porous beach and re-introducing the flow into the channel at the deep end between the wave paddle and the filter. Three flexible canvas hoses permitted re-introduction of flow with a minimum distortion of wave form.

An eleven meter long sand bed was placed in the central, horizontal portion of the channel, beginning about ten meters downwave from the wave maker. All measurements of wave height and velocity were made in this section of the channel. The wave channel had a glass wall midway along the sand bed, and centered around measurement station 5.5 meters. Measurement of the orbital trajectory of wave motion was made through the glass wall by observation of successive positions of neutrally buoyant particles in the water. Details of the trajectories were obtained by study of motion pictures of the particles. Velocity profiles, in the case of steady flow in the absence of waves, were obtained by use of a mini flow meter developed at the Hydraulic Research Station. Profiles of the rippled sand bed were obtained through the glass wall, and the rate of ripple advance determined by comparing successive ripple profiles.

A physical measure of the transport of sand was obtained from sand traps placed at the upwave and downwave ends of the sand bed. The traps consisted of perforated steel sheets placed flush with the level of the troughs of the sand ripples in the bed. The perforations consisted of slots ½ inch long by 1/16 inch wide and spaced 1/8 inch apart, arranged so that the ratio of solid to whole area was 0.77. The slots paralleled the orbital motion of the waves, and it was intended that sand carried over the traps by the wave motion, would fall through the slots and be retained in the void between the metal sheet and the cement floor of the channel.

Bed Material

The bed material consisted of quartz sand having a median diameter of about 0.2 millimeters. Mechanical analysis of the sand by sieves gave a median diameter of 0.19 mm while that by settling tube gave 0.22 mm. Both analyses gave a grain size distribution with a standard deviation σ_ϕ of about 0.35ϕ, where $\sigma_\phi = \log_2 [D_{16}/D_{84}]$ and D_{16} and D_{84} are the 16th and 84th percentile diameters of cumulative size distribution curve (Inman, 1952, table 1). The sand had a solid grain density ρ_s of 2.65 gm/cm^3 and a "dry" bulk density ρ_s' of 1.47 gm/cm^3, giving a volume concentration of 0.55.

EXPERIMENTAL PROCEDURE

Before each experiment the sand bed was smoothed by dragging a screen over the surface to obtain a uniform sand bed of about 4 cm thickness. Waves were then generated over the bed until the resulting sand ripples on the bed attained a constant and uniform height and length and a steady rate of advance. The wave maker was then stopped, water drained from the channel and the traps emptied of sand. Care was taken to replace any sand scoured from around the sand trap and to re-form the sand bordering the traps to a level such that the ripple troughs were approximately flush with the top of the perforated sheet forming the trap. The profile of the bed (measured to the ripple troughs) was then obtained and the channel refilled with water, ready for the experimental observation. A comparison of the bed profiles before and after Run 2C is shown in Figure 3.

The raw data from each experimental run is listed in Table 1. During each run, wave height profiles were obtained by hook-and-pointer gages over the 11 meter length of sand bed (Figures 5 and 6). Wave phase velocity, C, and wave period, T, were measured with a stop watch. The tabulated phase velocity has been reduced by the amount of the steady flow $\bar{u}$ upon which the wave train was riding. The volume discharge per unit time, Q, of the circulating water was measured with a manometer which gave the pressure difference across an orifice plate placed in the return-flow pipe; $\bar{u}$ was then given by Q/bh.

The orbital diameter of the wave motion near the bed, d_o, and the wave induced current over the bed, u_θ, were obtained by observing the trajectories of neutrally buoyant particles, called "Bagnold particles". These particles were made from a mixture of wax and lead stearate and had a median diameter of about 2 mm. Motion pictures were taken of their movement when close to the bed so that, by examining a series of frames, a diagram was obtained which showed the movement of water above the ripples during the passage of a wave, Figure 7. In most cases the orbital measurements apply to a zone about one half ripple wavelength above the bed, as the particle motion adjacent to the bed was too complex to obtain systematic measurements. The orbital diameter d_o is the mean of the horizontal components of upwave and downwave particle displacements, averaged over many wave cycles. The wave-drift current, u_θ, is the rate of drift of particles averaged over many wavelengths and includes drift induced by the steady current $\bar{u}$.

In the course of each run, fluorescent tracer grains were injected into the regime of sediment suspension above the bed. Twenty-one injections were made at 30 sec. intervals and the final tracer distribution in the

FLUME EXPERIMENTS ON SAND TRANSPORT BY WAVES AND CURRENTS

Table 1. Measurement over a rippled sand bed.

QUANTITY	SYMBOL	UNITS \ RUN	1A	1B	1C	1D	2A	2B	2C	2D
Superposed flow	$\tilde{U}$	cm/sec	0	2	4	6	0	2	4	6
Wave period	T	sec	1 4	1 4	1 4	1 4	2 0	2 0	2 0	2 0
Wave height	H	cm	15 7	15 3	15 1	15 4	16 5	16 5	16 8	16 8
Still water depth	h	cm	50 1	50 5	50 1	50 4	50 0	51 0	49 9	50 8
Wave phase velocity	C	cm/sec	180	183	187	184	206	209	205	209
Wavelength	L = CT	cm	254	258	264	259	412	418	410	416
Orbital diameter near bed	d_o	cm	9 8	9 4	9 6	9 6	19 2	18 5	18 6	18 2
Orbital velocity near bed	$u_m = \frac{\pi d_o}{T}$	cm/sec	21 8	21 0	21 4	21 4	30 1	29 1	29 2	28 6
Wave-drift current near bed	u_e	cm/sec	0 85	1 21	1 50	2 93	0 92	2 14	1 36	1 97
Water temperature		°C	8	7	6½	8½	15	11	6	7
Running time	Δt	min	98	62	50	70	44	44½	34	42
Downwave sand trap, dry wt		kg	4 76	4 54	3 83	2 93	3 68	5 28	2 56	3 23
Upwave sand trap, dry wt		kg	0 71	0 62	0 43	0 57	4 00	4 17	3 44	3 64
Ripple wavelength	λ	cm	6 5	6 5	6 5	6 4	10 8	10 2	10 6	10 3
Ripple height	η	cm	1 1	1 0	1 0	1 0	1 5	1 6	1 5	1 6
Ripple symmetry	β/λ	1	48	44	47	45	44	48	44	38
Rate of ripple advance	U_r	$10^{-3}\frac{cm}{sec}$	2 7	3 0	3 6	2 8	0 6	2 1	-2 5	-1 5
Wave height decrement	$\frac{\Delta H}{\Delta x}$	10^{-3}	1 64	1 46	1 55	1 73	1 00	1 00	1 22	1 33
Attenuation coefficient	a	$10^{-4} cm^{-1}$	1 02	0 93	0 99	1 17	0 60	0 61	0 72	0 78

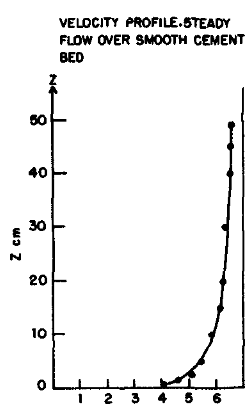

Z cm	u cm/sec
49 0	6 51
45 0	6.51
39 8	6.50
30 0	6.30
20 0	6.20
15 0	6.10
10 0	5 80
5.0	5.46
2.5	5.08
1 5	4 57
0 6	4 06

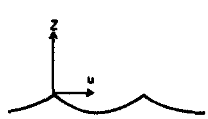

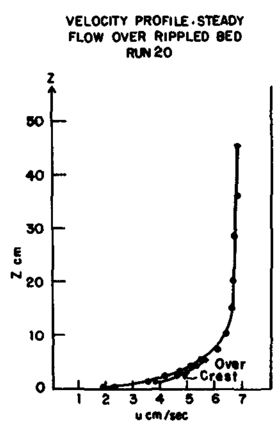

Z	Over Ripple Trough	Over Crest
0.5	2.0	3 8
1 5	3.5	4 6⁻
2 5	4 2⁺	5.0
3.5	4 7⁺	5.4
4 5	5.2	5 6⁺
5.5	5.5	
7 5	6.0	
10 5	6.4	
15.5	6.6⁺	
20.5	6 7	
28.5	6.8	
36.5	6.8	
45.0	6.8	

Fig. 4. Velocity profile for steady flow over smooth and rippled bed.

ripples is shown in Figure 8, for an experiment in which the ripple velocity was downwave. Methods to determine the rate of sediment transport are being developed and further interpretation of the tracer data may then be possible.

At the end of a run the flume was drained carefully, each trap was emptied and its sand content dried and weighed. Due to the decreases in wave height down the flume, the conditions above the two traps are not similar. A correction was made by assuming the transport into a trap was dependent on the power expended on the bed in that area. Putnam and Johnson (1949) suggest that the power expended on unit area of the bed can be approximated by taking the product of the bed stress, $c\rho u_m^2$ and the orbital velocity, u_m.

Then assuming trap content proportional to the power expended and hence to $c\rho u_m^3$, the content is proportional to u_m^3. The results given by the traps were corrected to give the quantity of sand which would have been caught if the traps had been subject to the wave conditions in the middle of the flume.

Four experiments were made in which the sand bed was replaced by a bed of smooth concrete. In each case the profile of the wave height was measured and the wave attenuation was assumed to be exponential (Eq. 6). Although the profile measured was confused due to the presence of standing waves, the general decrease in wave height closely approximated the expected exponential decrease and the value of the attenuation coefficient could be determined accurately.

Standing waves of wavelength approximately ½L were found in the wave height profile for every experiment whether over a sand or concrete bed. Ursell, Dean and Yu (1960) have thoroughly investigated this phenomenon which is due to the partial reflection of the propagating wave from the beach. No way was found to reduce the reflection coefficient to a value at which the standing waves would be of negligible amplitude.

In the early stages of a run the wave height at any given point varied due to the formation of the sand ripples on the bed which initially was smooth.

DISCUSSION

The attenuation coefficient for waves propagating in a smooth flume has been considered theoretically by Hunt (1952), Eq. 7, however the case of superimposed current was not considered. A comparison between the experimental and theoretical attenuation could only be made for runs 1A and 2A over a smooth concrete bed, Table 2. It can be seen that there was very good agreement between the measured values of attenuation of coefficient, $a_1 + a_2$ and the theoretical values, a_o. Theory also shows that, for the particular dimensions of channel used, the attenuation due to the walls alone was approximately $a_1 = 0.7\ a_o$, and that due to the smooth bed was $a_2 = 0.3\ a_o$. The wave attenuation due solely to the rippled bed should then be given by

$$a_3 = a - a_1 = a - 0.7(a_1 + a_2)$$

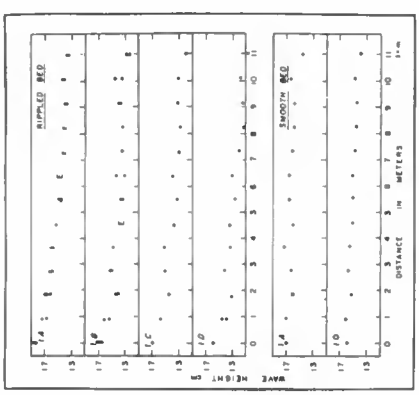

Fig. 5. Wave height profile for Run 1A - D.

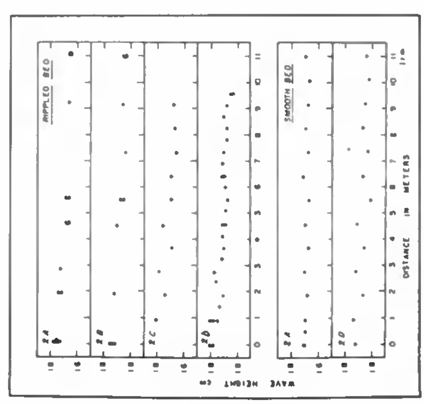

Fig. 6. Wave height profile for Run 2A - D.

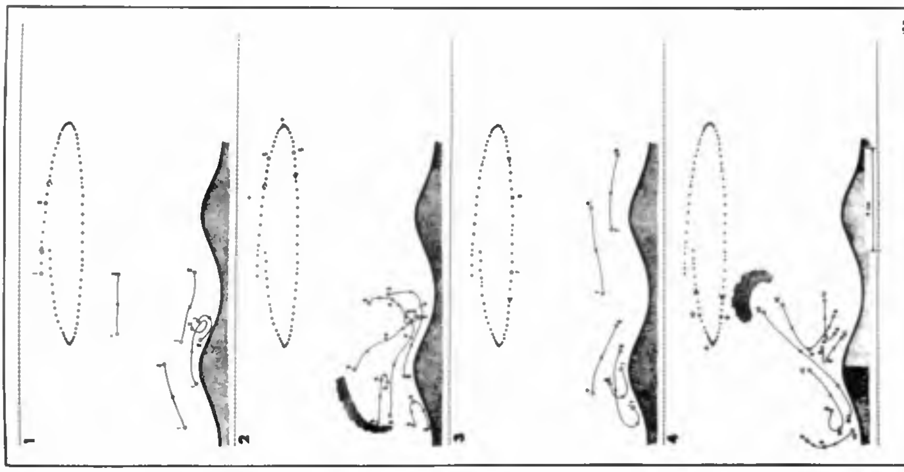

Fig. 7. Particle trajectories over a rippled bed.

The values of a_3 in Table 3 wer obtained using this correction. The value of a_3 was greatest for the runs with a short period, 1A - D, by an amount consistent with the attenuation being a "per wave" function.

Figure 7 shows the water movement over the ripple during the passage of a wave in run 1A. The water moving over a ripple crest during the forward semi-orbit generated a vortex in the lee of the ripple (1, 1-2). As the water decelerated, the system became unstable and the vortex, no longer restrained, dispersed rapidly. It was lifted up over the ripple by the combination of its own vorticity and the initial acceleration of the backward semi-orbit. This process removed sediment from above the downwave face of the ripple and dispersed it as a cloudy suspension moving upwave (2, 3-4-5). During the second half of the orbit a vortex was generated upwave from the ripple (3, 6-7) and then dispersed, its sediment content being thrown into suspension downwave from the ripple (4, 8-9-10). Material is thus placed in suspension, with some initial velocity, at two distinct periods during an orbit. If the motion were otherwise symmetrica the dirft velocity, u_θ, should then be the factor determining the directioı and magnitude of the sediment transport.

For runs 1A and 2A, which had no superimposed flow, the ripples were fairly symmetrical, but there was a considerable difference between the maximum height of the suspended sediment during the passage of a wave crest and that during the passage of a trough; the height being greater under a crest. The difference in height was approximately equal to the vertical orbital displacement.

The effect of the increase of $\bar{u}$ was to reduce further the symmetry of the system by increasing the effective orbital velocity downwave and decreasing it upwave. This resulted in a flattening of the upwave face of the ripple and the steepening of the downwave face. The vortex generated on the downwave face then became by far the stronger and hence much of the material placed in suspension had an upwave initial velocity. This mechanism was the cause of the negative ripple velocities found in runs 2 C, D and its general effect was to prevent an increase in u_θ necessarily increasing the sediment transport. It can be seen that for runs 1D and 2C the transport was less than for 1C and 2B despite an increase in $\bar{u}$. This can only be a temporary reversal as it is obvious that if $\bar{u}$ were considerably increased it would come to be more important than the wave motion and the transport would then be in the direction of the superimposed flow. Hence the increase in transport from 2C to 2D is not unexpected. However, the very high value of u_θ for run 2B was unexpected and unaccountable; otherwise the values of u_θ increased steadily for increasing $\bar{u}$, Figure 9.

Table 3 shows the values of the corrected transport rate of sand, j, the decrement in transmitted power of the waves attributable to bed drag, ω, and the coefficient of proportionality K as defined in Equation 2. For both series of experiments K was constant for increasing $\bar{u}$ as long as j increased also, i.e. as long as the system stayed reasonably symmetrical. However, when the system was subjected to periodic movements which were both strong and asymmetric, the basic assumptions of the energy theory were invalidated and the derived value of K decreased considerably.

Table 2. Measurement over a smooth concrete bed.

Wave height decrement	$\frac{\Delta H}{\Delta x}$	10^{-3}	0.50			0.64	0.29			0.55
Attenuation coefficient	a_1+a_2	$10^{-4}cm^{-1}$	0.30			0.40	0.17			0.33
Theoretical attenuation coefficient	a_o	$10^{-4}cm^{-1}$	0.28				0.18			

Table 3. Computations.

QUANTITY	SYMBOL	RUN / UNITS	1A	1B	1C	1D	2A	2B	2C	2D
Corrected downwave sand trap		10^{-2}gm/sec / cm width	1.38	2.12	2.29	1.42	2.41	3.08	2.24	2.16
Corrected upwave sand trap		10^{-2}gm/sec / cm width	0.18	0.20	0.17	0.17	2.06	2.24	2.35	1.98
Rate of sand transport	J	10^{-2}gm/sec / cm width	1.20	1.92	2.12	1.25	0.35	0.84	-0.11	0.18
Attenuation coefficient	a_3	$10^{-4}cm^{-1}$	0.81	0.70	0.74	0.89	0.48	0.46	0.53	0.55
Wave height decrement	$[\Delta H/\Delta X]_3$	10^{-3}	1.30	1.30	1.30	1.30	0.80	0.80	0.80	0.80
	$\frac{1}{4}gH(\Delta H/\Delta X)_3 Cn$	gm/sec^3	645	640	645	630	560	570	570	575
	$\frac{1}{4}gH(\Delta H/\Delta X)_3\bar{u}(2n+\frac{1}{2})$	gm/sec^3	--	19	37	55	--	14	29	43
Decrement in wave power	ω	gm/sec^3	645	659	682	685	560	584	599	618
Coefficient of proportionality	$K = \frac{I_\theta}{\omega}\frac{u_m}{u_\theta}$	---	0.29	0.30	0.27	0.08	0.12	0.12	-0.01	0.03
Transport by ripple advance	$0.37\rho_s'\lambda\eta U_r$	10^{-2}gm/sec / cm width	1.05	1.07	1.28	0.98	0.53	1.85	-2.15	-1.35

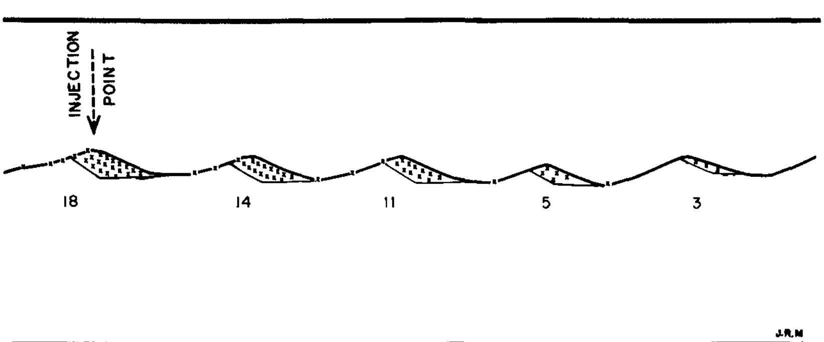

Fig. 8. Entrapment of tracer in ripple crest.

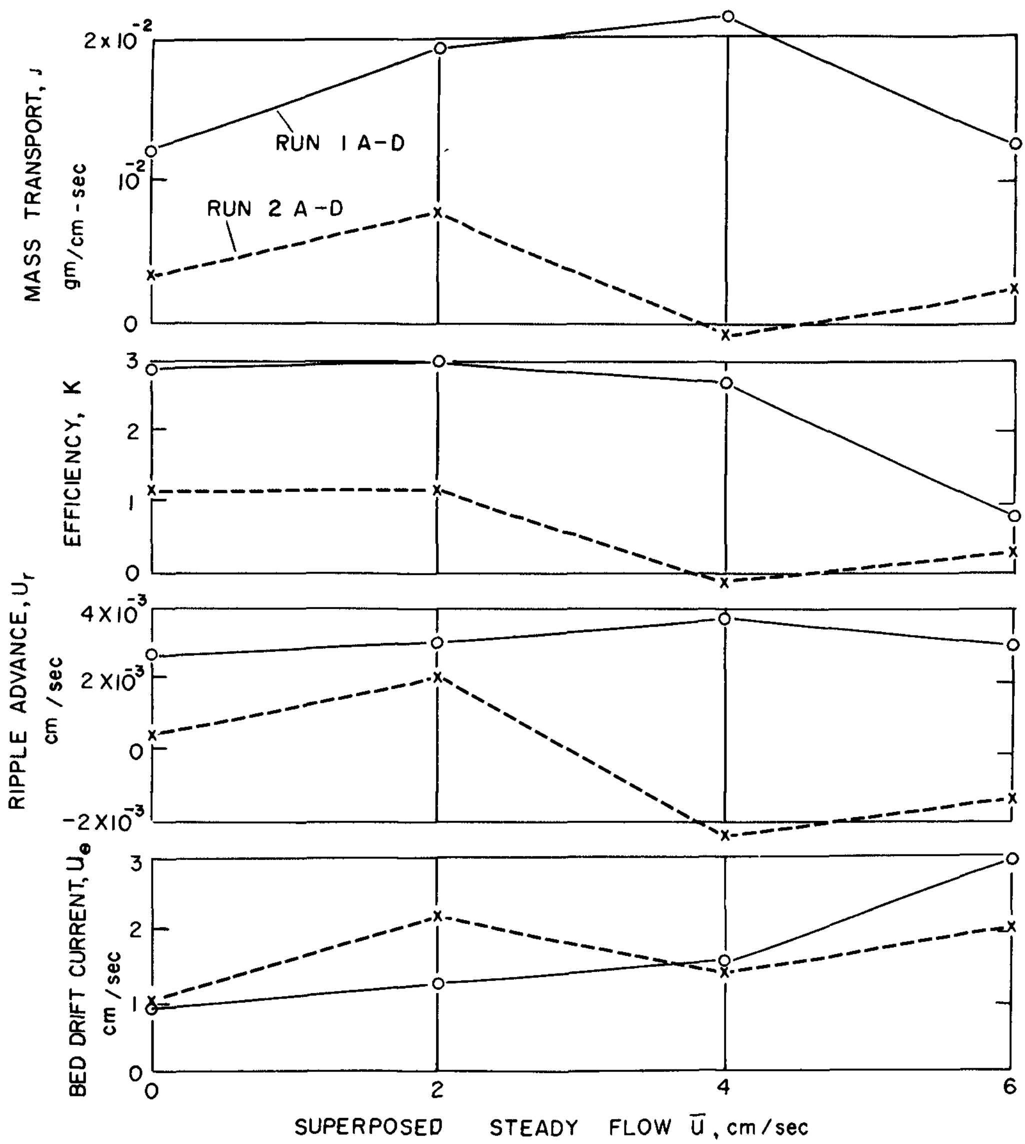

Fig. 9. Summary comparisons of transport properties of Runs 1 & 2.

It was determined that the area within the ripple profile was given by $0.37\lambda\eta$. The product of the mass of sand in a ripple and the rate of ripple advance $0.37\lambda\eta\rho_s \cdot U_r$ gave a transport expression which varied in much the same way as the measured sand transport.

FUTURE INVESTIGATIONS

This work comprises a pilot study and the conclusions drawn should be considered as tentative. The experiments should be repeated using a wider range of wave type, different sizes of bed sand, and wider, but controlled, conditions of liquid viscosity. It would be instructive to evaluate the transport relations when the orbital diameter greatly exceeds the ripple wavelength, causing the ripples to vanish and the bed to become smooth. Such a smooth bed is common near natural surf zones, and should be in better agreement with the model (Eq. 1).

Very little practical work has been done on the interaction between waves and currents, especially in the investigation of the behaviour of the boundary layer. For example, it is not known whether the superposition of wave motion on steady flow aids the spread of the turbulent boundary layer or inhibits it; or if the behaviour of the system depends on whether waves or currents are generated first. It would also be interesting to have complete vertical velocity profiles of the combined system, particularly for flow over ripples. It might then become possible to make a more direct comparison between the bahaviour of a beach and that of a model.

CONCLUSIONS

For low values of $\bar{u}$ a consistent relationship was found between the energy loss of the waves and the work done in transporting the sediment over the bed, the values of the coefficient, K, being 0.29 for run 1 and 0.12 for run 2. Further increase in $\bar{u}$ created a complex movement above the ripples which was periodic but asymmetric; the phase-dependent phenomena then had a greater effect on the system than that of the drift velocity. Under these conditions the theoretical assumptions were no longer valid and any calculated value of K was very small.

ACKNOWLEDGMENTS

The experimental work was performed at the Hydraulics Research Station, Wallingford, England, while the senior author was a Guggenheim Fellow. The authors are indebted to R. A. Bagnold for furnishing the guiding principles leading to this study. We wish to acknowledge the contributions of members of the Hydraulics Research Station staff; R. C. H. Russell, S. Yalin and H. Anwar for their many helpful suggestions during the course of the investigation; D. E. Newman for developing the tracers and an injection technique, and A. Lovegreen for modifying the experimental apparatus.

REFERENCES

Bagnold, R. A. (in press). Mechanics of marine sedimentation: The Sea, Ideas and Observations. (ed. by M. Hill, W. Munk, E. Goldberg and C. Iselin). Interscience Publishers.

Hunt, J. N. (1952). Viscous damping of waves over an inclined bed in a channel of finite width: La Houille Blanche, vol. 7, pp. 836-842.

Inman, D. L. (1952). Measures for describing the size distribution of sediments: Jour. Sed. Pet., vol. 22, pp. 125-148.

Longuet-Higgins, M. S. (1953). Mass transport in water waves: Phil. Trans. Royal Society, London, Series A, vol. 245, pp. 535-581.

Longuet-Higgins, M. S. and Stewart, R. W. (1960). Changes in the form of short gravity waves on long waves and tidal currents: Jour. Fluid Mechanics, vol. 8, pp. 565-583.

Putnam, J. A. and Johnson, J. W. (1949). The dissipation of wave energy by bottom friction: Trans. Amer. Geophys. Union, vol. 30, pp. 67-74

Russell, R. C. H. and Osorio, J. D. C. (1958). An experimental investigation of drift profiles in a closed channel: Proc. Sixth Conference Coastal Engineering, pp. 171-183.

Shepard, F. P. and Inman, D. L. (1950). Nearshore water circulation related to bottom topography and wave refraction: Trans. Amer. Geophys. Union, vol. 3, pp. 196-212.

Ursell, F.; Dean, R. G.; and Yu, Y. S. (1960). Forced small amplitude water waves: a comparison of theory and experiment: Jour. Fluid Mechanics, vol. 7, pp. 33-52.